Characterization of Phosphate Films on Aluminum Surfaces

B. Cheng, S. Ramamurthy, and N.S. McIntyre

A thin layer of phosphate conversion coating was formed on pure aluminum in a commercial zinc-manganese phosphating bath. A number of surface analytical techniques were used to characterize the phosphate thin films formed after immersion times ranging from 30 s to 10 min. The coating contained mainly a crystalline structure with dispersed micrometer-scale cavities. The major constituents of the phosphate film were zinc, phosphorus, and oxygen; a small amount of manganese was also detected. Based on these results, a three-stage mechanism was proposed for the formation and the growth of phosphate conversion coatings on aluminum. Electrochemical impedance spectroscopy was used to evaluate the corrosion performance of phosphated and uncoated aluminum samples in 0.50 *M* Na_2SO_4 and 0.10 *M* H_2SO_4 solutions. Both types of samples exhibited a passive state in the neutral solution and general corrosion behavior in the acid solution.

Keywords aluminum, coating, conversion, corrosion, growth, performance, phosphate

1. Introduction

Interest in using aluminum alloys in place of low-carbon steels for car body parts has grown in the automotive industry (Ref 1). The major reasons underlying this switch involve improvement of the overall energy efficiency of vehicles and of the corrosion resistance of the vehicle bodies (Ref 2). Such use of aluminum alloys often involves the application of paints for decoration and corrosion prevention. However, without proper surface modification, paints adhere poorly to these alloys.

Chemical conversion treatment in chromate (Ref 3-7) or chromate-phosphate (Ref 8-11) solutions has frequently been used to modify aluminum alloy surfaces in the past. However, chromate solutions have been widely associated with carcinogenesis (Ref 12, 13), and its removal as a waste is a problem. Current environmental legislation is moving toward a total ban on chromate-based treatments. Additionally, such treatments are not adaptable to the mixed steel-aluminum components frequently encountered in car body parts (Ref 14). Thus, there is a strong incentive to explore and evaluate alternative treatments for aluminum surface modification.

Recent studies (Ref 4, 15-18) have shown that chemical conversion treatment in chromate-free phosphate baths is a promising alternative for the surface modification of iron-aluminum components. It has long been recognized that phosphated metals exhibit substantially greater corrosion resistance and paint adhesion (Ref 19-21). More importantly, this technique has advantages over chromate-phosphate treatment in terms of environmental effects. Although a number of patents (Ref 22-29) pertaining to the phosphating of aluminum alloys are available and such processes are being used in the automotive industry, only a few mechanistic investigations (Ref 4, 15-18) have been reported to date.

B. Cheng, S Ramamurthy, and **N.S. McIntyre,** University of Western Ontario, London, Ontario, Canada N6A 5B7.

In general, the phosphating of metals can be described by the following processes:

$$M \rightarrow M^{n+} + ne \quad \text{(Eq 1)}$$

$$H_3PO_4 \rightarrow H^+ + H_2PO_4^- \rightarrow 2H^+ + HPO_4^{2-} \rightarrow 3H^+ + PO_4^{3-} \quad \text{(Eq 2)}$$

$$H^+ + e \rightarrow \frac{1}{2} H_2\uparrow \quad \text{(Eq 3)}$$

$$3M^{n+} + nPO_4^{3-} \rightarrow M_3(PO_4)_n \downarrow \quad \text{(Eq 4)}$$

For zinc and a number of steels, a metal is shown to dissolve in an acid solution to release metal ions; meanwhile, hydrogen evolves at the surface, which leads to an increase in pH and in the concentration of PO_4^{3-}. Metal ions combine with phosphate ions to form an insoluble phosphate film on the metal surface. It has been proven that the phosphating of zinc and steels follows this mechanism (Ref 19-21). If this mechanism were applied to the phosphating of aluminum alloys, aluminum phosphate conversion coatings might be expected to form on the aluminum surface. However, using x-ray diffraction (XRD), Ishii et al. (Ref 17) instead determined that the conversion coatings on aluminum are principally composed of tetrahydrated zinc phosphate (hopeite). The mechanistic conditions leading to this particular product on pure aluminum are of interest in the present work, which uses a number of surface analytical techniques, such as scanning electron microscopy/energy-dispersive x-ray analysis (SEM/EDX), x-ray photoelectron spectroscopy (XPS), and Auger electron spectroscopy (AES). In addition, electrochemical impedance spectroscopy (EIS) was used to characterize the corrosion behavior of phosphated aluminum in simulated environments.

2. Experimental

2.1 *Phosphating Procedure*

Specimens were prepared from pure aluminum foil of 99.997% purity (Johnson Matthey) with approximate dimensions of 10 by 5 by 0.1 mm. They were polished to a 600-grit finish, ultrasonically degreased in an acetone bath for 10 min, and dried in air. The samples were then cleaned in an alkaline cleaner (Parco cleaner 1520, Parker-Amchem Inc., Madison Heights, MI) for 4 min at 46 °C and rinsed with deionized water.

In accordance with aluminum phosphating procedure, the treated samples were predipped in a titanium colloidal solution (Parker-Amchem Inc.) at room temperature for 4 min. Then the predipped samples were immediately immersed in a proprietary phosphate bath (Parker-Amchem Inc.) at 46 °C, which was constantly stirred. This phosphate bath contains, among other constituents, a fluoride-based activation agent and a nitrite accelerator. Coatings were applied over a period of time ranging from 30 s to 10 min. The coated samples were then rinsed with deionized water, dried in air at room temperature, and stored in a desiccator.

2.2 *Surface Analyses*

The surface morphology and the coverage of the phosphate thin films on aluminum were observed using an ISI Cambridge Model DS-130 SEM (Cambridge Instruments) equipped with a Noran EDX. The acceleration voltage was 15 kV.

Surface analysis of the samples was performed using a Surface Science Laboratories model SSX-100 XPS. Survey spectra were obtained using an x-ray focused to a spot size of 600 μm. The spectrometer was initially calibrated using a pure gold sample, and the peak positions were similar to those published in the literature (Ref 30).

A Perkin-Elmer model PHI 600 AES was employed to characterize the compositions of various phases of phosphate film formed on aluminum. The Auger electron spectra was obtained using a 5 keV, 20 to 30 nA electron beam incident at 30° to the normal on the sample surface. The spectra were recorded in the EN(E) mode with a 1.2% resolution and were numerically differentiated for identification of peaks. The operating background pressures for both XPS and AES analyses were better than 1×10^{-6} Pa.

2.3 *Electrochemical Impedance Spectroscopy*

Electrochemical impedance spectra were measured for both phosphated and uncoated aluminum in a borate-buffered 0.50 *M* Na_2SO_4 solution (pH 7.8) and 0.10 *M* H_2SO_4 solution (pH ≈1) in order to evaluate the corrosion behavior of phosphated aluminum. The first solution represents a benign environment; the second solution simulates an acid-rain condition. The lowest pH value of acid rain recorded was 2.0 in the United States (Ref 31). The solutions were prepared in calibrated volumetric flasks using analytical-grade chemicals (Caledon Chemical Company) and deionized water (~18 MΩ cm). Prior to the immersion of a sample, the solutions were deaerated for at least 1 h.

The EIS measurements were carried out in a conventional three-electrode cell at room temperature (23 ± 1 °C) using a home-built potentiostat and a frequency response analyzer (Solartron model 1255), which were interfaced to a personal computer. A saturated calomel electrode (SCE) was utilized as the reference electrode, and a platinum sheet with an approximate surface area of 10 cm^2 was used as the counterelectrode. The samples acted as working electrodes, with exposed areas of about 1 cm^2.

The uncoated samples were polished to a 600-grit finish prior to impedance measurements, and the coated samples were analyzed in the as-coated condition. The samples were rinsed with deionized water prior to immersion in the cell containing deaerated solutions. The open circuit potential (E_{corr}) was allowed to stabilize for about 1 h before an EIS measurement. A small sinusoidal alternating voltage of 10 mV_{P-P} with a frequency ranging from 50 kHz to 1 mHz was applied to the working electrode, and the resultant current response was recorded. To ensure reproducibility, the measurements were repeated at least twice.

3. Results and Discussion

3.1 *Surface Analysis*

Scanning electron micrographs of the films formed on pure aluminum in the phosphating bath after various immersion times are shown in Fig. 1(b) to (f). For comparison, the surface morphology of a sample after polishing and predipping but prior to immersion in the bath is shown in Fig. 1(a); the surface is rough, with the polishing scratches clearly detectable. Figure 1(b) indicates that only small, spongelike particles were present on the aluminum surface after about 30 s of immersion. At longer immersion times, the spongelike particles transformed into distinct crystals and grew rapidly (Fig. 1c and d), which indicates that the sponges are the precursors of phosphate crystals. It is clear that only a short incubation time is required for phosphate film to form on aluminum. This process is different from that observed in the phosphating of zinc and steels. Gaarenstroom and Ottaviani (Ref 32) showed that there are no apparently distinct stages in the phosphating of these metals.

Figure 1(d) shows that more than 90% surface area was covered by the formed crystals after an immersion of 2 min. On further immersion, film growth slowed somewhat, but the coverage of crystals on the aluminum surface continued to increase until a thin layer of uniform, complete conversion coating with a flaky crystalline structure was formed after 5 min of immersion (Fig. 1d and e). The coating morphology shown in Fig. 1(e) indicates that the phosphate film contained randomly dispersed micrometer-scale cavities (indicated by arrows). These cavities could potentially improve the adhesion of subsequent paint layers by providing locations for mechanical "keying" of molecules; however, they could also reduce the corrosion resistivity of phosphated aluminum.

Figures 1(e) and (f) show that further increases in immersion time did not significantly improve the coverage of phosphate film on aluminum. In fact, these microcavities cannot be

eliminated completely. From a practical viewpoint, a 5 min immersion is sufficient to produce a thin layer of phosphate conversion coating on aluminum.

The EDX analyses (Table 1) indicated that the composition of the crystals was quite different from that of the spongelike particles. The crystals appeared to be enriched in zinc, phos-

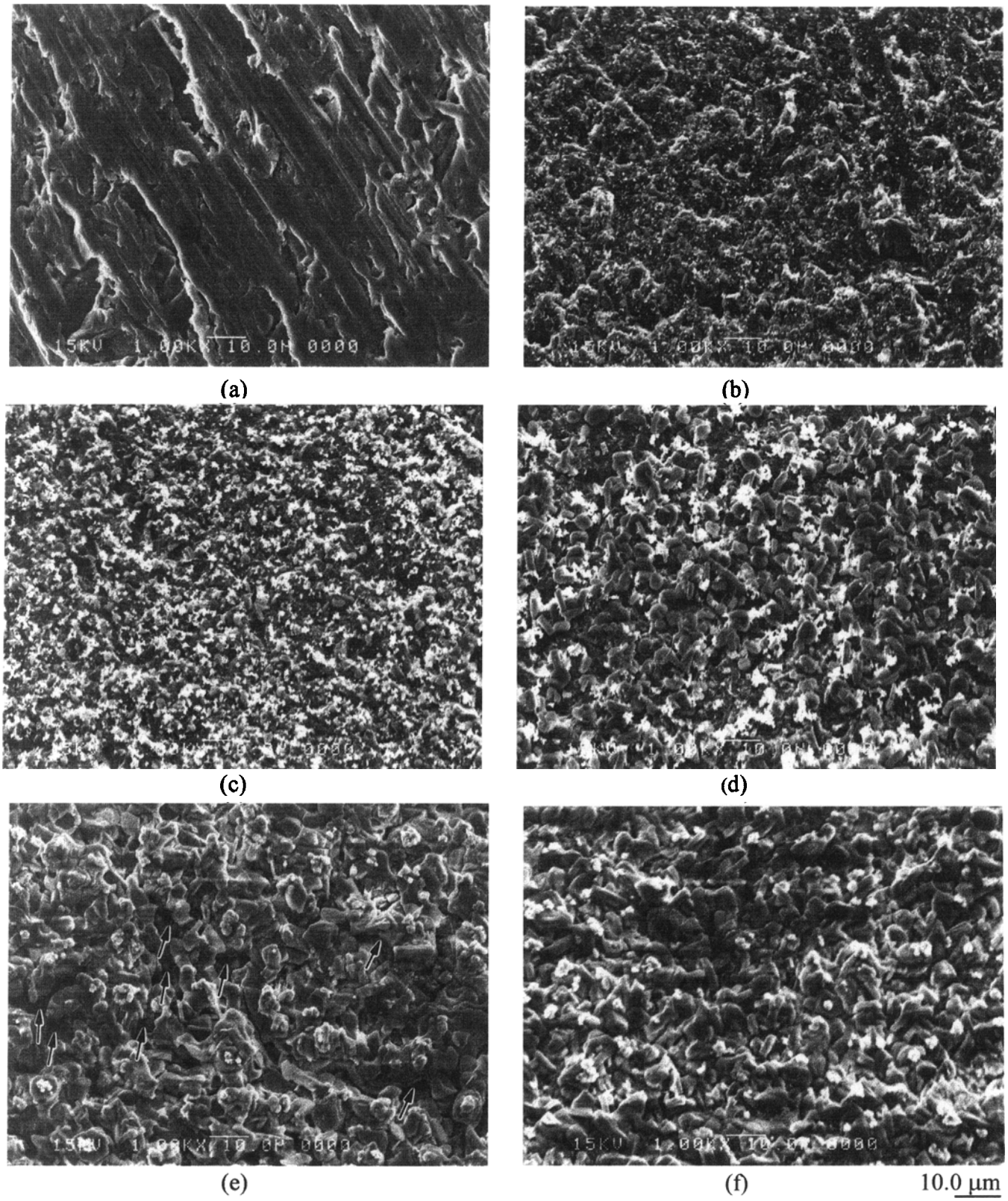

Fig. 1 SEM images of aluminum samples immersed in the phosphating bath for various periods. (a) Before immersion. (b) 30 s. (c) 1 min. (d) 2 min. (e) 5 min. (f) 10 min

phorus, and oxygen; a small amount of manganese was also detected. In contrast, zinc and aluminum were the dominant constituents of the spongelike particles. These results also support the notion that distinguished stages do exist in the phosphating process of aluminum.

To clarify the distinct stages, AES was used to analyze the surface compositions of the sponges, crystals, and substrate. This technique can provide information on the composition of layers only a few atoms thick within a very small spot size (<0.05 μm). The EDX method, by contrast, gives the average composition of the outer 1 to 2 μm thickness of the sample surface.

Typical AES spectra for the sponges, crystals, and substrate are shown in Fig. 2. The exposed substrate exhibited strong AES peaks for aluminum, oxygen, and carbon and weak peaks for zinc and phosphorus (Fig. 2a). The spongelike particles contained zinc, oxygen, carbon, and a small amount of phosphorus (Fig. 2b). The crystals exhibited a much greater amount of phosphorus (Fig. 2c). The carbon peaks present in three spectra could result from contamination when samples were exposed to air and hence were not included in the quantification procedure. Table 2 summarizes the compositions of the sponges, crystals, and substrate from AES analyses.

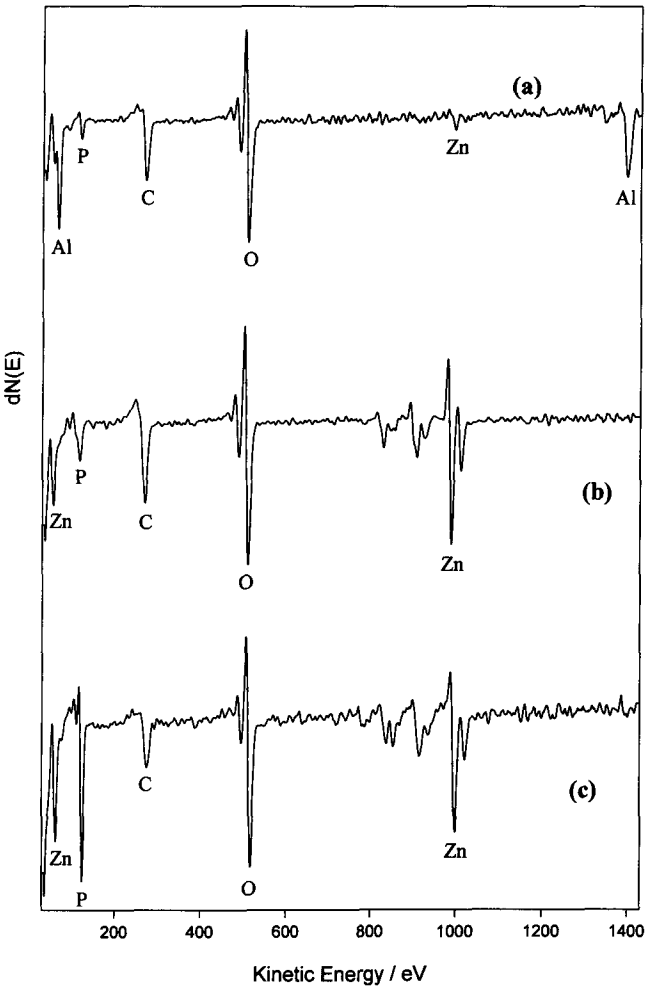

Fig. 2 AES spectra of sponges and crystals formed on an aluminum surface in the phosphating bath. (a) Aluminum substrate. (b) Sponges. (c) Crystals

The results of the AES analyses were generally consistent with those of the EDX analyses, except for the nonappearance of aluminum in the sponges. Presumably, aluminum detected by EDX analysis of the sponges arose from the substrate. Small amounts of phosphorus were detected by both AES and EDX. The phosphorus may result from the precipitation of zinc phosphate from the bulk solution or the partial phosphatization of deposited zinc. Zinc was found to be a major component of the sponges. This can be explained only if the sponges were formed by the substitution reaction of zinc for aluminum on fresh aluminum surface in the phosphating bath. In order for such a substitution reaction to take place, the aluminum surface must first be cleaned of its native oxide film. This could occur through its chemical dissolution in the presence of fluoride ions. Typically, passive aluminum in a pH 3.1 phosphate solution containing 0.02 *M* free F^- can be cleaned of oxide ("activated") within an immersion period of approximately 15 s (Ref 33). The resultant substituted zinc sponges rapidly oxidize in air. This accounts for the substantial amount of oxygen on the sponges detected by AES and EDX.

The composition of the crystals as determined by AES and EDX agrees with the results of Ishii et al. (Ref 17). Using XRD, these authors suggested that the composition of the phosphate coating on an aluminum-magnesium alloy was $Zn_3(PO_4)_2$, not $AlPO_4$. This is in contrast to the phosphate films on zinc and iron, which are mainly composed of $Zn_3(PO_4)_2$ and $FePO_4$, respectively.

On the basis of the preceding discussion, it is suggested that the phosphating of aluminum takes place in at least three

Table 1 EDX analysis of compositions of substrate, sponges, and crystals on aluminum surfaces

Element, at.%	Substrate	Sponges	Crystals
Oxygen	3.4	5.6	43.1
Aluminum	83.7	24.1	0.6
Phosphorus	0.9	0.7	24.3
Silicon	1.2	2.6	0.2
Titanium	...	0.2	...
Manganese	...	...	4.0
Nickel	1.0	0.8	0.9
Zinc	9.8	66.1	27.0

Note: Carbon was rejected in quantitatively calculating the compositions because carbon was thought to be contamination resulting from the atmosphere during sample transfer.

Table 2 AES analysis of compositions of substrate, sponges, and crystals on aluminum surfaces

Element, at.%	Substrate	Sponges	Crystals
Oxygen	40.6	34.9	31.4
Aluminum	46.5	...	...
Phosphorus	4.4	6.1	22.6
Zinc	8.5	59.0	46.0

Note: Carbon was rejected in quantitatively calculating the compositions because carbon was thought to be contamination resulting from the atmosphere during sample transfer.

stages: (1) a short incubation period with activation of passive aluminum and substitution of zinc for aluminum, leading to the deposition of zinc sponges onto fresh aluminum surface; (2) a fast growth stage where the deposited zinc sponges grow into zinc phosphate crystals, along with the rapid growth of individual crystals; and (3) a final stage in which the surface coverage increases, leading to the eventual formation of a thin layer of uniform phosphate coating.

X-ray photoelectron spectroscopy can provide information on surface composition for the coating as a whole due to a relatively large incident x-ray beam size. To identify the changes on the aluminum surface during the phosphating process, XPS was used to characterize the surface composition of the samples after three different treatment steps: (1) after polishing to a 600-grit finish and alkaline cleaning, (2) after predipping in a titanium colloidal solution, and (3) after phosphating immersion for 5 min. Survey spectra collected from these samples are presented in Fig. 3.

Aside from some surface carbon contamination, only aluminum oxide was detected after alkaline cleaning (Fig. 3a). Small potassium and silicon peaks were also observed, which could result from the residue of the alkaline cleaner. After the predipping (Fig. 3b), in addition to aluminum and oxygen, the surface film contained sodium and phosphorus; the latter may result from colloidal particles of $Na_4TiO(PO_4)_2$ adsorbed onto the aluminum surface during predipping. Tegehall (Ref 34) suggested that the sodium ions present on the surface of the titanium phosphate particles exchange with zinc ions in the subsequent phosphating process and thereafter act as nucleation sites. As in previous investigations (Ref 32, 34), titanium was not observed in our study. As shown in Fig. 3(c), after phosphating, the composition of the phosphate film is similar to those obtained from EDX and AES analyses. Aluminum was not observed in the phosphate thin film, suggesting a reasonably complete coverage of zinc phosphate film on the aluminum surface.

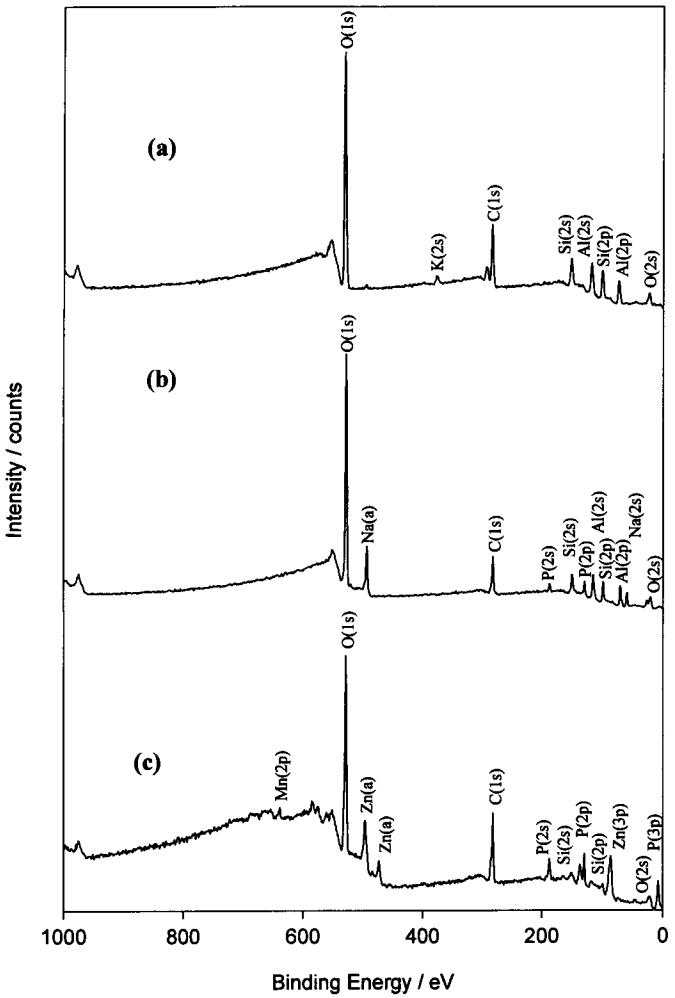

Fig. 3 XPS survey scan spectra for aluminum samples after different treatments. (a) Before predipping. (b) After predipping. (c) After 5 min immersion in phosphating bath

3.2 *Corrosion Behavior of Phosphated Aluminum*

In the borate-buffered 0.5 *M* Na_2SO_4 aqueous solution, the impedance spectra for both coated and uncoated aluminum exhibited a typical capacitive feature, as shown in Fig. 4 (where both Bode and Nyquist formats are presented). The polarization resistance (R_P) values were estimated to be about 10^5 Ω cm^2 for both phosphated and uncoated samples. The high polarization resistance corresponds to a high corrosion resistivity, indicating that both phosphated and uncoated aluminum are in a passive state in a neutral environment.

In contrast, the impedance spectra for both coated and uncoated aluminum were relatively intricate in the acid solution (0.1 *M* H_2SO_4). As shown in Fig. 5(b), the spectra consisted of

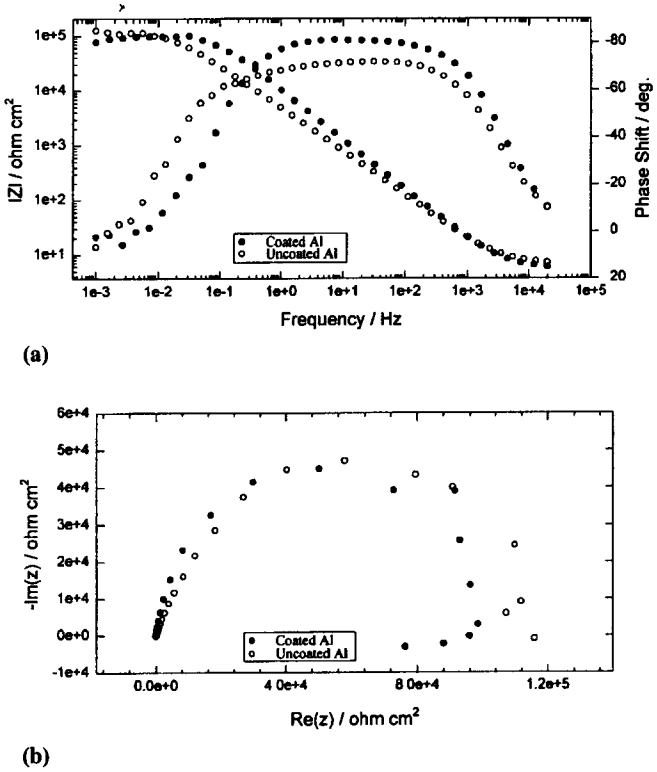

Fig. 4 EIS spectra of coated and uncoated aluminum in borate-buffered 0.50 *M* Na_2SO_4 aqueous solution at room temperature (~23 °C). (a) Bode plot. (b) Nyquist plot

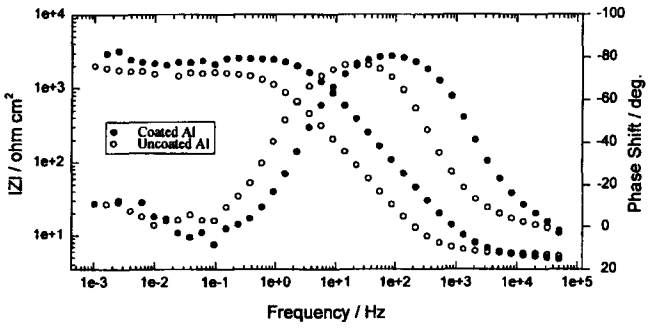

(a)

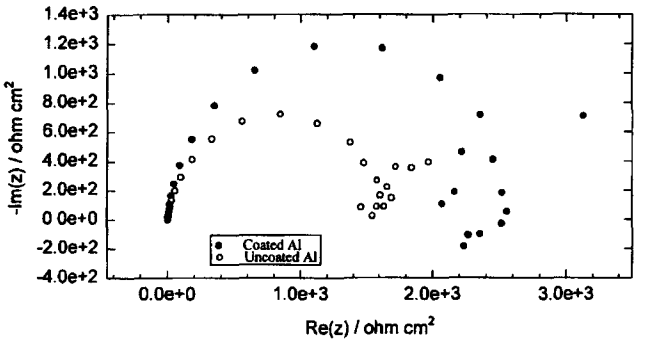

(b)

Fig. 5 EIS spectra of coated and uncoated aluminum in 0.10 *M* H_2SO_4 aqueous solution at room temperature (~23 °C). (a) Bode plot. (b) Nyquist plot

two parts: a capacitive loop occurring in relatively high-frequency region and an inductive loop present in a low-frequency region. The spectra from this study are in good agreement with those obtained in previous studies (Ref 35-39). Cao (Ref 40) suggested that these types of spectra could be described by the equivalent circuit in Fig. 6 under the following conditions: $A < 0$, $B > 0$, and $D - R_t|A| > 0$. The parameters A, B, and D are related to the properties of a corrosion system in Eq 5 to 7:

$$|A| = \frac{R_C(R_t + R_L) - R_t^2}{R_t^2 R_C CL} \quad \text{(Eq 5)}$$

$$B = \frac{R_t^2 C - L}{R_t^2 CL} \quad \text{(Eq 6)}$$

$$D = \frac{R_t R_L + R_L R_C + R_t R_C}{R_t R_C CL} \quad \text{(Eq 7)}$$

where C and L are the apparent capacitance and inductance of the corresponding electrode, respectively; R_t represents the charge transfer resistance; and R_C and R_L stand for the current-leaking resistances of the capacitance and inductance, respectively. Accordingly, the polarization resistance can be expressed by:

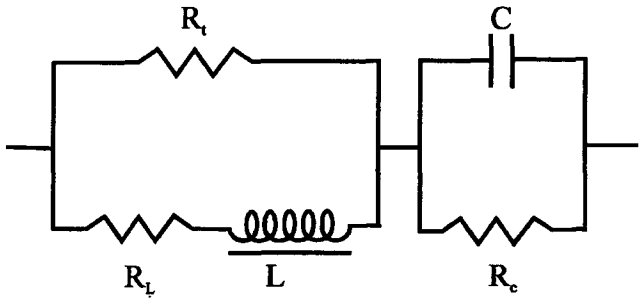

Fig. 6 Equivalent circuit corresponding to EIS spectra of phosphated and uncoated aluminum in the acid solution

$$R_P = \frac{R_t D}{D - R_t|A|} \quad \text{(Eq 8)}$$

It was estimated that the polarization resistances for coated and uncoated aluminum in 0.1 *M* H_2SO_4 solution were approximately $2.2 \times 10^3\ \Omega \cdot cm^2$ and $1.5 \times 10^3\ \Omega \cdot cm^2$, respectively. These values are two orders of magnitude lower than those observed in the neutral medium, which indicates that both the coated and uncoated aluminum samples in 0.10 *M* H_2SO_4 solution undergo general corrosion. This is understandable because the phosphate conversion coating and the native oxide film on uncoated aluminum are soluble in the acid solution:

$$Zn_3(PO_4)_2 \cdot 4H_2O + H^+ \rightarrow Zn^{2+} + HPO_4^{2-} + H_2O \quad \text{(Eq 9)}$$

$$Al_2O_3 + H^+ \rightarrow Al^{3+} + H_2O \quad \text{(Eq 10)}$$

However, the coated aluminum exhibited slightly better corrosion resistance than uncoated aluminum.

Despite the differences in spectroscopic parameters between phosphated and uncoated samples, the characteristics of their impedance spectra were identical. The time constant at high frequencies can be attributed to the interfacial reactions — for example, aluminum being oxidized to aluminum ions. The existence of an inductance in the corrosion system, however, is difficult to explain. Generally, the inductive feature in electrochemical impedance spectra accounts for a rearrangement of surface charge at the metal/film interface or ionic diffusion through the barrier film on the metal surface (Ref 35, 36).

Low polarization resistance for phosphated aluminum in 0.10 *M* H_2SO_4 suggests that the phosphate coating alone is unlikely to provide sufficient corrosion protection for aluminum in acid media. Posttreatments, such as subsequent painting operations, filler materials, passivation, and anodization, are required to provide additional protection against corrosion. An alternative method is to modify the formulation of current phosphate baths so that more corrosion-resistant phosphate thin films can be obtained.

4. Summary

The phosphating process of aluminum includes at least three sequential stages: (1) an incubation period of about 30 s

after immersion, in which the native oxide film on aluminum surface dissolves and zinc substitutes for aluminum to form zinc sponges depositing on the fresh aluminum surface; (2) a growth stage within 2 min of immersion, where the zinc sponges transform into zinc phosphate crystals and grow rapidly, coupled with evolution of hydrogen and reduction of the accelerators in the phosphating bath; and (3) a final stage that occurs within 5 min of immersion, in which the individual crystals continue to grow, but relatively slowly, to form a uniform and complete film covering the aluminum substrate.

The phosphate conversion coatings on aluminum are principally composed of zinc, phosphorus, oxygen, and a small amount of manganese in the form of a crystalline structure with dispersed micrometer-scale cavities. This is in good agreement with results from previous studies (Ref 15-17) in which the phosphate conversion coatings on aluminum were found to be, in fact, tetrahydrated zinc phosphate (hopeite).

Like passive aluminum, the phosphated aluminum has a high corrosion resistance in a neutral aqueous solution. Although both uncoated and coated aluminum exhibited a general corrosion behavior in the acid solution, the coated aluminum exhibited a slightly better corrosion resistance than the uncoated aluminum due to the buffering role of phosphates.

References

1. R. Gopal and D.W. Gibbons, Report of the Electrolytic Industries for the Year 1993, *J. Electrochem. Soc.*, Vol 141 (No. 10), 1994, p 2918-2933
2. H.N. Han and J.P. Clark, Lifetime Costing of Body-in-White: Steel vs. Aluminum, *J. Met.*, Vol 47 (No. 5), 1995, p 22-28
3. S. Wernick and R. Pinner, *The Surface Treatment and Finishing of Aluminum and Its Alloys: Including the Production of Aluminum Coatings for Protection,* 4th ed., Draper Publishers, Teddington, England, 1972, p 233-290
4. S.M. Cohen, Review: Replacements for Chromium Pretreatments on Aluminum, *Corrosion,* Vol 51 (No. 1), 1995, p 71-78
5. F.W. Lytle, R.B. Greegor, G.L. Bibbins, K.Y. Blohowiak, R.E. Smith, and G.D. Tuss, An Investigation of the Structure and Chemistry of a Chromium-Conversion Surface Layer on Aluminum, *Corros. Sci.,* Vol 37 (No. 3), 1995, p 349-369
6. G.M. Brown, K. Shimizu, K. Kobayashi, G.E. Thompson, and G.C. Wood, The Morphology, Structure and Mechanism of Growth of Chemical Conversion Coatings on Aluminum, *Corros. Sci.,* Vol 33 (No. 9), 1992, p 1371-1385; The Development of Chemical Conversion Coatings on Aluminum, *Corros. Sci.,* Vol 35 (No. 1-4), 1993, p 253-256
7. J.A. Treverton and M.P. Amor, High-Resolution SEM Studies of Chromate Conversion Coatings, *J. Mater. Sci.,* Vol 23, 1988, p 3706-3710
8. J.A. Treverton, M.P. Amor, and A. Bosland, Topographical and Surface Chemical Studies of Chromate-Phosphate Pretreatment Films on Aluminum Surfaces, *Corros. Sci.,* Vol 33 (No. 9), 1992, p 1411-1426
9. B. Shadzi, Chromium Phosphate for Aluminum, *Met. Finish.,* Vol 87 (No. 10), 1989, p 41-43
10. S. Spring and K. Woods, Prepaint Treatments—Chromate Coatings, *Met. Finish.,* Vol 79 (No. 6), 1981, p 49-55
11. J.W. Davis, Surface Analysis of Conversion Coatings on Aluminum and Steel, *Org. Coat. Plast. Chem.,* Vol 43, 1980, p 507-512
12. P.A. Schweitzer, *Corrosion and Corrosion Protection Handbook,* Marcel Dekker, 1988, chap. 4
13. J.W. Bibber, A Chromium-Free Conversion Coating for Aluminum, *Met. Finish.,* Vol 91 (No. 12), 1993, p 46-47
14. S. Wernick and R. Pinner, *The Surface Treatment and Finishing of Aluminum and Its Alloys,* ASM International, 1987, p 220-260
15. T. Foster, G.N. Blenkinsop, P. Blattler, and M. Szandorowski, Development of a Chromate-Free Primer for Aluminum and Steel to Meet CGSB Specifications, *J. Coat. Technol.,* Vol 63 (No. 801), 1991, p 101-110
16. W.F. Heung, Y.P. Yang, P.C. Wong, K.A.R. Mitchell, and T. Foster, XPS and Corrosion Studies on Zinc Phosphate Coated 7075-T6 Aluminum Alloy, *J. Mater. Sci.,* Vol 29, 1994, p 1368-1373, 3653-3657
17. H. Ishii, O. Furuyama, and S. Tanaka, Phosphating Treatment for Car Bodies with Aluminum Alloy Parts, *Met. Finish.,* Vol 91 (No. 4), 1993, p 7-10
18. J.F. Ying, M.Y. Zhou, B.J. Flinn, P.C. Wong, K.A.R. Mitchell, and T. Foster, The Effect of Ti-Colloid Surface Conditioning on the Phosphating of 7075-T6 Aluminum Alloy, *J. Mater. Sci.,* Vol 31, 1996, p 565-571
19. I. Suzuki, *Corrosion-Resistant Coatings Technology,* Marcel Dekker, 1989
20. D.B. Freeman, *Phosphating and Metal Pre-Treatment: A Guide to Modern Process and Practice,* 1st ed., Industrial Press, New York, NY, 1986
21. G. Lorin, *Phosphating of Metals,* Finishing Publications, Middlesex, U.K., 1974
22. M. Nakatsukasa, N. Miyazaki, and Y. Yoshida, Method and Treating Solution for Phosphating Metal Surfaces, Japanese Patent 90-67989, 16 March 1990
23. I. Kawasaki, M. Ishinda, A. Mochizuki, and H. Kojima, Method for Treating Metal Surface with Zinc Phosphate, Japanese Patent 91-113572, 18 May 1991
24. M.S. Boulos, Fluoride-Containing Bath for Conversion Coating of Aluminum Alloys, U.S. Patent 93-146242, 1 Nov 1993
25. S. Ikeda and S. Meguro, Conversion Coating Bath Containing Rare-Earth Metal Salts in Surface Treatment of Aluminum Alloy Articles, Japanese Patent 89-199656, 1 Aug 1989
26. H. Ishii and A. Yoshida, Pretreatment of Aluminum Materials or Aluminum-Coated Steels Prior to Painting, Japanese Patent 92-293746, 7 Oct 1992
27. R. Wolf-achim, J.W. Brouwer, K.H. Gottwald, B. Mayer, and K. Brands, Phosphating with Nickel- and Copper-Free Acidic Solutions, German Patent 93-4330104, 6 Sept 1993
28. M. Matsuo and T. Kobayashi, Phosphating of Aluminum Alloy Sheets for Automobiles, Japanese Patent 92-200395, 3 July 1992
29. K. Sato, Y. Myazaki, O. Furuyama, A. Mochizuki, and H. Kojima, Continuous Phosphating Treatment of Steel-Aluminum Alloy Composites, Japanese Patent 92-35175, 21 Feb 1992
30. D. Briggs and M.P. Seah, *Practical Surface Analysis,* 2nd ed., Vol 1, John Wiley & Sons, 1990, p 535
31. J.R. Luoma, *Troubled Skies, Troubled Water—The Story of Acid Rain,* Viking Press, 1984, p 31
32. S.W. Gaarenstroom and R.A. Ottaviani, Characterization of Phosphate Crystal Nucleation and Growth on Cold-Rolled Steel, *J. Vac. Sci. Technol. A,* Vol 6 (No. 3), 1988, p 966-970
33. B. Cheng, N.S. McIntyre, and S. Ramamurthy, "Mechanism of Formation of the Phosphate Conversion Coatings on Pure Aluminum," Poster, 8th Canadian Materials Science Conf. (London, Ontario), 11-15 June 1996
34. P.-E. Tegehall, Colloidal Titanium Phosphate, the Chemical Activator in Surface Conditioning before Zinc Phosphating, *Colloids Surf.,* Vol 42, 1989, p 155-164; The Mechanism of Chemical Activation with Titanium Phosphate Colloids in the Formation of Zinc Phosphate Conversion Coatings, *Colloids Surf.,* Vol 49, 1990, p 373-383
35. H.J.W. Lenderink, M.V.D. Linden, and J.H.W. de Wit, Corrosion of Aluminum in Acidic and Neutral Solutions, *Electrochim. Acta,* Vol 38 (No. 14), 1993, p 1989-1992

36. J.H.W. de Wit and H.J.W. Lenderink, Electrochemical Impedance Spectroscopy as a Tool to Obtain Mechanistic Information on the Passive Behavior of Aluminum, *Electrochim. Acta,* Vol 41 (No. 7/8), 1996, p 1111-1119

37. C.M.A. Brett, The Application of Electrochemical Impedance Techniques to Aluminum Corrosion in Acidic Chloride Solution, *J. Appl. Electrochem.,* Vol 20, 1990, p 1000-1003

38. J.B. Bessone, D.R. Salinas, C.E. Mayer, M. Ebert, and W.J. Lorenz, An EIS Study of Aluminum Barrier-Type Oxide Films Formed in Different Media, *Electrochim. Acta,* Vol 37 (No. 12), 1992, 2283-2290

39. J. Bessone, C. Mayer, K. Jüttner, and W.J. Lorenz, AC-Impedance Measurements on Aluminum Barrier-Type Oxide Films, *Electrochim. Acta,* Vol 28 (No. 2), 1983, p 171-175

40. C.-N. Cao, On the Impedance Plane Displays for Irreversible Electrode Reactions Based on the Stability Conditions of the Steady-State, Part II: Two State Variables Besides Electrode Potential, *Electrochim. Acta,* Vol 35 (No. 5), 1990, p 837-844